

Nonlocal Kondo effect and two-fluid picture revealed in an exactly solvable model

Jiangfan Wang¹ and Yi-feng Yang^{1,2,3,*}

¹*Beijing National Laboratory for Condensed Matter Physics,
Institute of Physics, Chinese Academy of Sciences, Beijing 100190, China*

²*School of Physical Sciences, University of Chinese Academy of Sciences, Beijing 100190, China*

³*Songshan Lake Materials Laboratory, Dongguan, Guangdong 523808, China*

(Dated: January 31, 2023)

Understanding the nature of local-itinerant transition of strongly correlated electrons is one of the central problems in condensed matter physics. Heavy fermion systems describe the f -electron delocalization through Kondo interactions with conduction electrons. Tremendous efforts have been devoted to the so-called Kondo-destruction scenario, which predicts a dramatic local-to-itinerant quantum phase transition of f -electrons at zero temperature. On the other hand, two-fluid behaviors have been observed in many materials, suggesting coexistence of local and itinerant f -electrons over a broad temperature range but lacking a microscopic theoretical description. To elucidate this fundamental issue, here we propose an exactly solvable Kondo-Heisenberg model in which the spins are defined in the momentum space and the \mathbf{k} -space Kondo interaction corresponds to a highly nonlocal spin scattering in the coordinate space. Its solution reveals a continuous evolution of the Fermi surfaces with Kondo interaction and two-fluid behaviors similar to those observed in real materials. The electron density violates the usual Luttinger's theorem, but follows a generalized one allowing for partially enlarged Fermi surfaces due to partial Kondo screening in the momentum space. Our results highlight the consequence of nonlocal Kondo interaction relevant for strong quantum fluctuation regions, and provide important insight into the microscopic description of two-fluid phenomenology in heavy fermion systems.

I. INTRODUCTION

Underlying the rich emergent quantum phenomena of heavy fermion systems^{1,2} is the local-to-itinerant transition of f -electrons controlled by the interplay of Kondo and Ruderman-Kittel-Kasuya-Yosida (RKKY) interactions³⁻¹⁵. Below the so-called coherence temperature T^* , a large amount of experimental observations have pointed to the coexistence of local and itinerant characters of f -electrons as captured phenomenologically by the two-fluid model¹⁶⁻²², which assumes the coexistence of an itinerant heavy electron fluid formed by hybridized (screened) f -moments and a (classical) spin liquid of residual unhybridized f -moments. The two-fluid behavior exists over a broad temperature range, from the normal state below the coherence temperature down to inside the quantum critical superconducting phase²³⁻²⁵, and explains a variety of anomalous properties observed in heavy fermion materials²². But a microscopic description of the two-fluid phenomenology is still lacking, and no consensus has been reached on how exactly the f -electrons become delocalized²⁶.

Tremendous theoretical and experimental efforts in past decades have been focused on the so-called Kondo-destruction scenario, in which the local-itinerant transition was predicted to occur abruptly through a quantum critical point (QCP) at zero temperature⁴⁻⁶. While it seems to be supported experimentally by the Hall coefficient jump under magnetic field extrapolated to zero temperature in YbRh₂Si₂²⁷ and the de Haas-van Alphen experiment under pressure in CeRhIn₅²⁸, it was lately challenged by a number of angle-resolved photoemission spectroscopy measurements showing signatures

of large Fermi surfaces²⁹ or band hybridization above the magnetically ordered state³⁰. In theory, the Kondo-destruction scenario could be derived under certain local or mean-field approximations, such as the dynamical large- N approaches assuming independent electron baths coupled to individual impurity^{9,10,14} and the extended dynamical mean-field theory by mapping the Kondo lattice to a single impurity Bose-Fermi Kondo model⁴. Since the corresponding spin- $\frac{1}{2}$ single- or two-impurity problems only allow for two stable fixed points in the strong-coupling limit and the decoupling limit³¹⁻³³, these approaches unavoidably predicted a single QCP associated with Kondo destruction.

However, there is no a priori reason to assume such a local impurity mapping to be always valid for Kondo lattice systems in which all spins are spatially correlated and coupled to a common shared bath. For example, in CePdAl³⁴, geometric frustration may promote quantum fluctuations of local spins so that the single QCP is replaced by an intermediate quantum critical phase at zero temperature^{11,12}. Numerically, density-matrix renormalization group (DMRG) calculations of the one-dimensional (1D) Kondo lattice have predicted an intermediate phase with neither large nor small Fermi surfaces³⁵. For 2D Kondo lattice, both quantum Monte Carlo (QMC) simulations^{36,37} and the dynamical cluster approach³⁸ have suggested continuous existence of Kondo screening inside the magnetic phase. In particular, an effective nonlocal Kondo interaction has recently been proposed using an improved Schwinger boson approach with full momentum-dependent self-energies, yielding intermediate ground states with partially enlarged electron Fermi surfaces^{11,12,39}. It is therefore necessary to go be-

yond the local or mean-field approximations and explore in a more rigorous manner how f -electrons may evolve once nonlocal interaction effects are taken into account.

In this work, we extend the concept of Kondo interaction to an extreme case where the nonlocal scattering between conduction electrons and spins has an infinite interacting range such that it becomes local in the momentum space. We further include a Heisenberg-like term in the momentum space to mimic the Kondo-RKKY competition in heavy fermion materials. Similar to the Hatsugai-Kohmoto model with a \mathbf{k} -space Hubbard- U interaction^{40–44}, our proposed \mathbf{k} -space Kondo-Heisenberg model is exactly solvable. This allows us to overcome uncertainties in previous studies introduced by either analytical approximations or numerical ambiguities and extract decisive information on potential physical effects of nonlocal correlations. We find many interesting features such as spin-charge separated excitations, coexistence of Kondo singlets and spin singlets, and continuous evolution of the Fermi surfaces. Our results yield useful insight into the microscopic description of two-fluid behaviors, highlight the rich consequences of nonlocal Kondo scattering, and provide an unambiguous counterexample to the local Kondo-destruction scenario.

II. RESULTS

A. The \mathbf{k} -space Kondo-Heisenberg model

We begin by constructing the following Hamiltonian,

$$H = \frac{1}{2} \sum_{\mathbf{k}} H_{\mathbf{k}},$$

$$H_{\mathbf{k}} = (\epsilon_{\mathbf{k}} - \mu)(n_{\mathbf{k}} + n_{-\mathbf{k}}) + J_K(\mathbf{s}_{\mathbf{k}} \cdot \mathbf{S}_{\mathbf{k}} + \mathbf{s}_{-\mathbf{k}} \cdot \mathbf{S}_{-\mathbf{k}}) + J_H \mathbf{S}_{\mathbf{k}} \cdot \mathbf{S}_{-\mathbf{k}}, \quad (1)$$

where $n_{\mathbf{k}} = \sum_{\alpha} c_{\mathbf{k}\alpha}^{\dagger} c_{\mathbf{k}\alpha}$ is the electron occupation number at momentum \mathbf{k} , μ is the chemical potential, and $\epsilon_{\mathbf{k}} = \epsilon_{-\mathbf{k}}$ is the electron dispersion relation. The electron spin $\mathbf{s}_{\mathbf{k}} = \frac{1}{2} \sum_{\alpha\beta} c_{\mathbf{k}\alpha}^{\dagger} \boldsymbol{\sigma}_{\alpha\beta} c_{\mathbf{k}\beta}$ and the local spin $\mathbf{S}_{\mathbf{k}}$ are both defined in the momentum space. Note that $\mathbf{S}_{\mathbf{k}}$ is not the Fourier transform of the spin operator in the coordinate space, but should rather be viewed as that of an “ f -electron” localized in the momentum space. In the pseudofermion representation, this corresponds to $\mathbf{S}_{\mathbf{k}} = \frac{1}{2} \sum_{\alpha\beta} f_{\mathbf{k}\alpha}^{\dagger} \boldsymbol{\sigma}_{\alpha\beta} f_{\mathbf{k}\beta}$ under the constraint $\sum_{\alpha} f_{\mathbf{k}\alpha}^{\dagger} f_{\mathbf{k}\alpha} = 1$. It is immediately seen that the Kondo interaction is highly nonlocal by Fourier transform to the coordinate space, $\frac{J_K}{2} \sum_{ijj'j'} c_{i\alpha}^{\dagger} c_{j\beta} f_{j'\alpha}^{\dagger} f_{j'\beta} \delta_{\mathbf{r}_i - \mathbf{r}_j, \mathbf{r}_{j'} - \mathbf{r}_{i'}}$. A similar form of nonlocal Kondo interaction has been suggested to emerge in the quantum critical regime and play an important role in strongly frustrated Kondo systems^{11,12,39}.

The above model is exactly solvable, since the total Hilbert space can be divided into many small and independent subspaces by each conserved $H_{\mathbf{k}}$. The local

Hilbert space at each momentum point contains 8 states constructed by 4 electron states ($|0\rangle, |\uparrow\rangle, |\downarrow\rangle, |2\rangle$) and 2 spin states ($|\uparrow\rangle, |\downarrow\rangle$), so $H_{\mathbf{k}}$ has a total number of 64 eigenstates and can be exactly diagonalized. These states are further classified into different sectors by the electron numbers $(n_{\mathbf{k}}, n_{-\mathbf{k}})$. Depending on the relative magnitudes of $\epsilon_{\mathbf{k}} - \mu$ and $\zeta \equiv (J_K - J_H + \tilde{J})/4$, where $\tilde{J} = \sqrt{J_H^2 - 2J_H J_K + 4J_K^2}$, we may find the ground state of $H_{\mathbf{k}}$ among three possibilities: 1) for $\epsilon_{\mathbf{k}} - \mu > \zeta$, one has $(n_{\mathbf{k}}, n_{-\mathbf{k}}) = (0, 0)$, and $\mathbf{S}_{\mathbf{k}}, \mathbf{S}_{-\mathbf{k}}$ form a spin singlet; 2) for $|\epsilon_{\mathbf{k}} - \mu| < \zeta$, $(n_{\mathbf{k}}, n_{-\mathbf{k}}) = (1, 1)$, and the ground state is a superposition between Kondo singlets and spin singlets, as shown in Table I and Fig. 1(c); 3) for $\epsilon_{\mathbf{k}} - \mu < -\zeta$, one has $(n_{\mathbf{k}}, n_{-\mathbf{k}}) = (2, 2)$, and the two \mathbf{k} -local spins form a singlet. Other sectors like $(n_{\mathbf{k}}, n_{-\mathbf{k}}) = (0, 1)$ and $(1, 2)$ only contribute to excited states (see *Appendix A*). The momentum space is therefore separated into three different regions, Ω_0, Ω_1 and Ω_2 , corresponding to $n_{\mathbf{k}} = 0, 1, 2$, as illustrated in Figs. 1(a) and 1(b). The ground state of H is simply a direct product of the above three states at different \mathbf{k} .

Many interesting properties arise from the existence of the singly occupied region Ω_1 , which seems to be a general feature of models with \mathbf{k} -space local interactions^{40,45–47}. The volume of Ω_1 , defined as $V_{\Omega_1} = \frac{1}{\mathcal{N}} \sum_{\mathbf{k}} \theta(\zeta - |\epsilon_{\mathbf{k}} - \mu|)$ where \mathcal{N} is the total number of \mathbf{k} points, is shown in Fig. 1(d), which maps out the phase diagram on the J_H - J_K plane. For simplicity, we have assumed $\epsilon_{\mathbf{k}} = k^2/2\pi - 1$, $\mu = 0$, and $\epsilon_{\mathbf{k}} - \mu \in [-1, 1]$. The momentum average is then $\frac{1}{\mathcal{N}} \sum_{\mathbf{k}} \equiv \int_{|\mathbf{k}| < k_{\Lambda}} d^2\mathbf{k}/(2\pi)^2$, where $k_{\Lambda} = 2\sqrt{\pi}$ is the momentum cutoff corresponding to a Brillouin zone volume $(2\pi)^2$. At $J_K = 0$, one has $V_{\Omega_1} = 0$, and the conduction electrons are completely decoupled from the “ \mathbf{k} -space valence bond state” formed by the local spins⁴⁷, hence the name decoupled metal. For J_K and J_H satisfying $\zeta \geq 1$ (below the white curve in Fig. 1(d)), one has $V_{\Omega_1} = 1$, such that all spins are Kondo screened by conduction electrons. This is the Kondo insulator (KI) phase with an insulating gap around the

\mathbf{k}	$(n_{\mathbf{k}}, n_{-\mathbf{k}})$	$E_{\mathbf{k}}$	Ground State
$\epsilon_{\mathbf{k}} - \mu > \zeta$	(0,0)	$-\frac{3}{4}J_H$	$ 00\rangle \otimes \text{SS}\rangle$
$ \epsilon_{\mathbf{k}} - \mu < \zeta$	(1,1)	$2(\epsilon_{\mathbf{k}} - \mu) - \frac{J_K + \tilde{J}}{2} - \frac{J_H}{4}$	$a \text{KS}\rangle_{\mathbf{k}} \otimes \text{KS}\rangle_{-\mathbf{k}} + b \text{ss}\rangle \otimes \text{SS}\rangle$
$\epsilon_{\mathbf{k}} - \mu < -\zeta$	(2,2)	$4(\epsilon_{\mathbf{k}} - \mu) - \frac{3J_H}{4}$	$ 22\rangle \otimes \text{SS}\rangle$

TABLE I: The ground states of $H_{\mathbf{k}}$. $E_{\mathbf{k}}$ is the ground state energy. $|00\rangle$ and $|22\rangle$ denote the empty and fully occupied electron states at \mathbf{k} and $-\mathbf{k}$. $|\text{ss}\rangle$ ($|\text{SS}\rangle$) denotes the spin singlet formed by the two electrons (local spins) at \mathbf{k} and $-\mathbf{k}$, while $|\text{KS}\rangle_{\mathbf{k}}$ denotes the Kondo singlet at \mathbf{k} . The ratio between the coefficients a and b is $2J_K/(J_H + \tilde{J} - 2J_K)$.

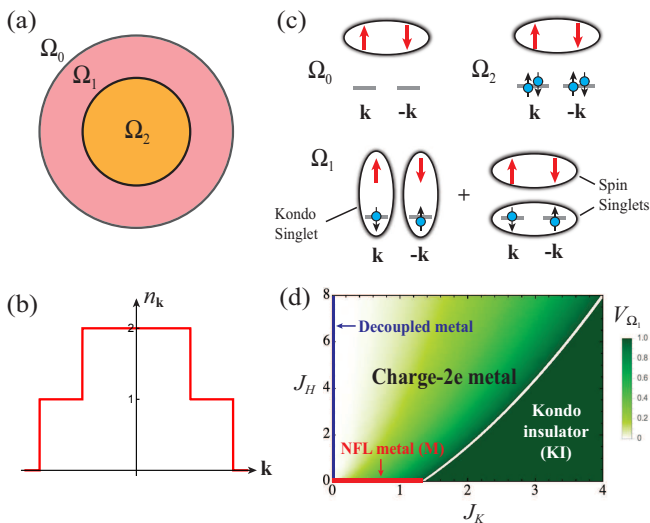


FIG. 1: The ground state of \mathbf{k} -space Kondo-Heisenberg model. (A) The momentum space contains three regions with different electron occupation number shown in (B). (C) Ground states of $H_{\mathbf{k}}$ in each momentum region. The red arrows and blue balls with a black arrow denote the local spins and conduction electrons, respectively. The ellipses represent the entangled Kondo singlet or spin singlet. (D) The ground state phase diagram at $\mu = 0$, showing different phases. The color represents the volume of the singly occupied region Ω_1 .

Fermi energy. In between, one has $0 < V_{\Omega_1} < 1$, and the system is in a charge- $2e$ metal with gapped single-particle excitations but gapless two-particle (Cooper pair) excitations. As one approaches the $J_H = 0$ limit from inside the charge- $2e$ metal, the single particle gap vanishes, and the system becomes a non-Fermi liquid (NFL) metal, which we denote as M.

B. Excitations

The elementary excitations can be obtained exactly from the single-particle retarded Green's function defined as $G_c(\mathbf{k}, t) = -i\theta(t) \langle \{c_{\mathbf{k}\alpha}(t), c_{\mathbf{k}\alpha}^\dagger\} \rangle$. Its explicit analytical expression at zero temperature is given in *Appendix B*. The poles of the Green's function are plotted in Fig. 2(a) in different phases, with the spectral weights represented by the thickness of the curves. Two additional poles in the Ω_1 region are not shown as they have very small weights and locate far away from the Fermi energy. For $\zeta < 1$, the following poles are most close to the Fermi energy:

$$\begin{aligned} \omega_{0,\mathbf{k}} &= \epsilon_{\mathbf{k}} - \mu - \frac{J_K - 2J_H + 2\tilde{J}'}{4}, & \mathbf{k} \in \Omega_0 \\ \omega_{1,\mathbf{k}}^\pm &= \epsilon_{\mathbf{k}} - \mu \pm \frac{J_K + 2\tilde{J}' - 2\tilde{J}'}{4}, & \mathbf{k} \in \Omega_1 \\ \omega_{2,\mathbf{k}} &= \epsilon_{\mathbf{k}} - \mu + \frac{J_K - 2J_H + 2\tilde{J}'}{4}, & \mathbf{k} \in \Omega_2 \end{aligned} \quad (2)$$

where $\tilde{J}' = \sqrt{J_H^2 - J_H J_K + J_K^2}$. Physically, $\omega_{0,\mathbf{k}}$ corresponds to adding one electron at $\mathbf{k} \in \Omega_0$, so that the system is excited from the state $|00\rangle \otimes |\text{SS}\rangle$ to one of the lowest doublets of the $(n_{\mathbf{k}}, n_{-\mathbf{k}}) = (1, 0)$ sector, for example, $C_1 |\text{KS}\rangle_{\mathbf{k}} \otimes |\downarrow\rangle_{-\mathbf{k}} + C_2 |\text{SS}\rangle \otimes |\downarrow\rangle_{\mathbf{k}}$ if the added electron has a down spin (see Fig. 2(b)). Interestingly, the component $|\text{KS}\rangle_{\mathbf{k}} \otimes |\downarrow\rangle_{-\mathbf{k}}$ creates a charge $-e$ excitation (anti-holon⁴⁵) at \mathbf{k} and a spin-1/2 excitation (spinon) at $-\mathbf{k}$, while the component $|\text{SS}\rangle \otimes |\downarrow\rangle_{\mathbf{k}}$ creates an electron excitation at \mathbf{k} . The former indicates spin-charge separated excitations that dominate at small J_H/J_K due to the vanishing weight $|C_2|^2$ in the $J_H \rightarrow 0$ limit as shown in Fig. 2(c). Similarly, the pole $\omega_{1,\mathbf{k}}^-$ corresponds to removing one electron at $\mathbf{k} \in \Omega_1$, and the resulting excited state is a superposition between a hole excitation at \mathbf{k} (with coefficient C_1), and a holon-spinon pair located at opposite momentum points (with coefficient C_2). The poles $\omega_{1,\mathbf{k}}^+$ and $\omega_{2,\mathbf{k}}$ have similar physical meanings, but with the empty states in Fig. 2(b) replaced by the double-occupied states.

In the charge- $2e$ metal, as shown in Fig. 2(a), the poles $\omega_{0,\mathbf{k}}$ and $\omega_{1,\mathbf{k}}^-$ are separated by a direct energy gap at the Ω_0 - Ω_1 boundary, and the same for $\omega_{1,\mathbf{k}}^+$ and $\omega_{2,\mathbf{k}}$ at the Ω_1 - Ω_2 boundary. We find the gap follows a scaling function $\Delta/J_K = \frac{1}{2}[z + (z^2 - 2z + 4)^{1/2} - 2(z^2 - z + 1)^{1/2}]$, with $z = J_H/J_K$. It vanishes in the limit $J_H \rightarrow 0$, leading to two ‘‘Fermi surfaces’’ in the M phase, as denoted by FS1 and FS2 in Fig. 2(a). However, these are not usual electron Fermi surfaces, in the sense that moving an electron from one side of the Fermi surface to the other causes spin-charge separation. Therefore, the M phase at $J_H = 0$ is actually a NFL metal. We will see that even for $J_H > 0$, the physics should be qualitatively identical to the M phase at temperatures higher than the single particle gap of the charge- $2e$ metal ground state.

Inside the KI phase, both Ω_0 and Ω_2 disappear, and the single particle gap becomes an indirect gap between $\omega_{1,\mathbf{k}}^+$ and $\omega_{1,\mathbf{k}}^-$. This gap remains open in the $J_H \rightarrow 0$ limit, and has a different nature from that of the charge- $2e$ metal. Their difference becomes more clear when we consider the two-particle Green's function, $G_b(\mathbf{k}, t) = -i\theta(t) \langle [b_{\mathbf{k}}(t), b_{\mathbf{k}}^\dagger] \rangle$, where $b_{\mathbf{k}}^\dagger = \frac{1}{\sqrt{2}}(c_{\mathbf{k}\uparrow}^\dagger c_{-\mathbf{k}\downarrow}^\dagger - c_{\mathbf{k}\downarrow}^\dagger c_{-\mathbf{k}\uparrow}^\dagger)$ creates a singlet pair of electrons (a Cooper pair)⁴⁶. As shown in Fig. 2(d), $G_b(\mathbf{k}, \omega)$ is gapped in the KI phase but gapless in the charge- $2e$ metal. This means, inside the charge- $2e$ metal, adding or removing a singlet pair of electrons at \mathbf{k} and $-\mathbf{k}$ costs no energy if \mathbf{k} locates exactly at the Ω_0 - Ω_1 or Ω_1 - Ω_2 boundaries, indicating Cooper pairs rather than electrons being its elementary charge carriers. However, because our simple model does not contain scatterings between Cooper pairs, this state can only be viewed as a completely quantum disordered superconductor without long-range phase coherence^{47,48}.

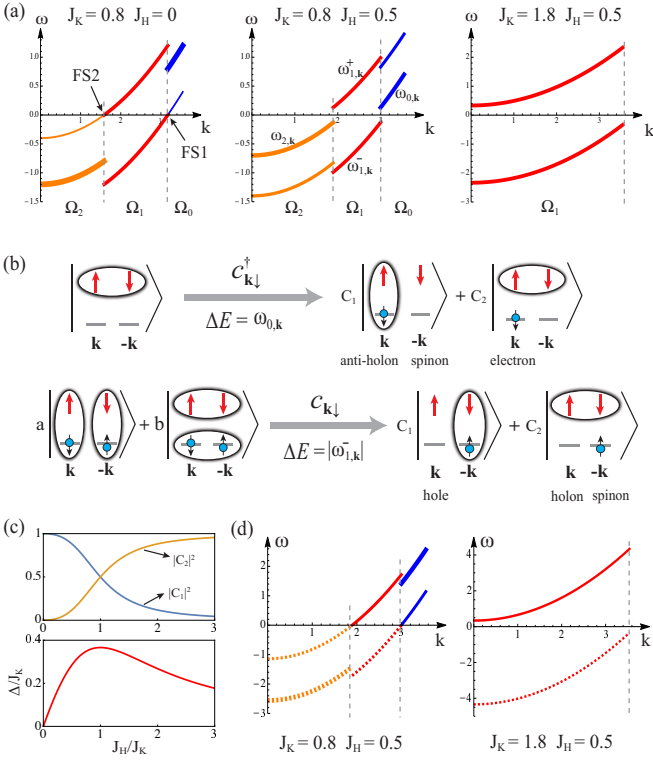


FIG. 2: Low-energy excitations. (A) The poles of the single particle Green's function at $\mu = 0$ for three typical values of J_K and J_H corresponding to the M (left), charge- $2e$ metal (middle) and KI (right) phases. The blue, red and orange curves represent the excitations with momentum $\mathbf{k} \in \Omega_0$, Ω_1 and Ω_2 , respectively, and the thickness of the curves is proportional to the spectral weight of the poles. (B) The physical meanings of the poles $\omega_{0,\mathbf{k}}$ and $\omega_{1,\mathbf{k}}$. (C) The coefficient C_1 and C_2 (up) and the single particle gap (bottom) as functions of J_H/J_K in the charge- $2e$ metal phase. (D) The poles of the two-particle Green's function in the charge- $2e$ metal (left) and KI (right) phases. The dashed curves correspond to the poles with negative spectral weights.

C. Two-fluid behavior

The fact that the ground state involves a superposition of the Kondo singlets and local spin singlets in the momentum space is reminiscent of the two-fluid model of heavy fermion materials, in which an “order parameter” $f(T) = \min\{1, f_0(1 - T/T^*)^{3/2}\}$ was found to characterize the fraction of hybridized f -moments over a broad temperature range, with f_0 reflecting the strength of collective hybridization (or collective Kondo entanglement)^{18,20}. $f_0 \geq 1$ indicates full screening below some characteristic temperature where $f(T)$ reaches unity, while $0 < f_0 < 1$ implies that a fraction of f -electrons may remain unhybridized even down to zero temperature if the scaling is not interrupted by other orders. The two-fluid model captures a large amount of experimental properties of heavy fermion metals²², but its microscopic theory remains to be explored²⁶.

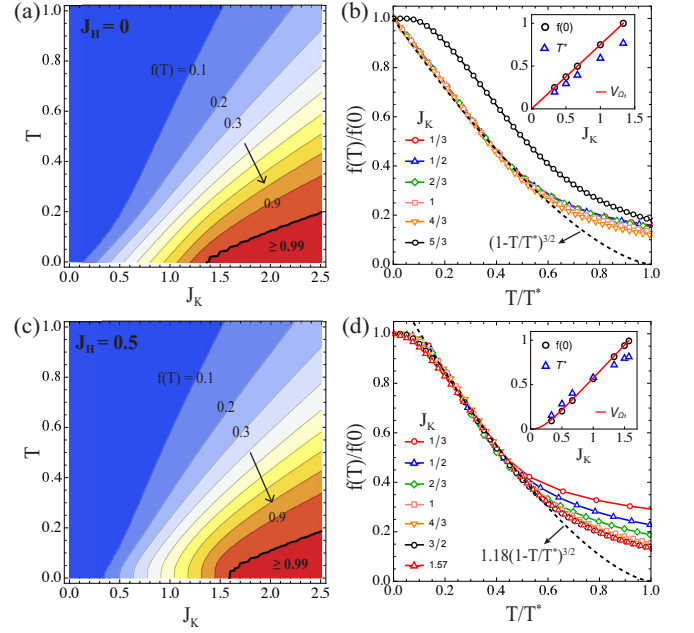


FIG. 3: The two-fluid “order parameter”. (A) A contour plot of the two-fluid “order parameter” $f(T)$ for $J_H = 0$. (B) $f(T)/f(0)$ as a function of T/T^* for $J_H = 0$ and different J_K . The dashed curve shows the phenomenological scaling function $(1 - T/T^*)^{3/2}$ for comparison. The inset shows $f(0)$, T^* , and V_{Ω_1} as functions of J_K . (C)(D) The same as (A)(B), but with $J_H = 0.5$. The dashed curve in (D) corresponds to $1.18(1 - T/T^*)^{3/2}$.

To see how two-fluid behavior may emerge in our exactly solvable model, we introduce the projector $P_{\mathbf{k}} = |\mathbf{K}\rangle\langle\mathbf{K}|$ with $|\mathbf{K}\rangle = \frac{1}{2}(|\uparrow\downarrow\rangle - |\downarrow\uparrow\rangle)_{\mathbf{k}}(|\uparrow\downarrow\rangle - |\downarrow\uparrow\rangle)_{-\mathbf{k}}$, and its momentum average $P = \frac{1}{\mathcal{N}} \sum_{\mathbf{k}} P_{\mathbf{k}}$. This gives a two-fluid “order parameter”,

$$f(T) = \frac{\text{Tr}[e^{-H/T} P]}{\text{Tr}[e^{-H/T}]} = \frac{1}{\mathcal{N}} \sum_{\mathbf{k}} \frac{\text{Tr}[e^{-H_{\mathbf{k}}/T} P_{\mathbf{k}}]}{\text{Tr}[e^{-H_{\mathbf{k}}/T}]}, \quad (3)$$

which reflects the fraction of Kondo singlet formation in the momentum space. With this definition, it is easy to show that a physical observable can in principle also be divided into a two-fluid form $\langle O \rangle = f\langle O \rangle_P + (1 - f)\langle O \rangle_{1-P}$.

Figures 3(a) and 3(c) show the contour plots of the calculated $f(T)$ at $J_H = 0$ and 0.5 , respectively. In general, we see $f(T)$ increases with decreasing temperature and saturates to a finite zero temperature value $f(0)$. For $J_H = 0$, $f(0)$ increases linearly from 0 to 1 with increasing J_K , and stays at unity for $J_K > 4/3$ (inside the KI phase). For $J_K < 4/3$ (inside the M phase), $f(T)$ follows a universal scaling function $f(T)/f(0) = F(T/T^*)$, as shown in Fig. 3(b). Quite remarkably, the low temperature part of $F(T/T^*)$ can be well approximated by the function $(1 - T/T^*)^{3/2}$. At high temperatures, its smooth evolution reflects a crossover rather than a phase transition of the delocalization with temperature. For

$J_K > 4/3$, $f(T)$ grows to unity already at a finite temperature, in good agreement with the expectation of the two-fluid picture²⁰. The results for $J_H = 0.5$ are slightly different. We find for small J_H , $f(T)$ already stays constant below certain temperature before it reaches unity. This is due to the energy gap of the charge- $2e$ metal that interrupts the two-fluid scaling. Above the gap, $f(T)$ follows the same two-fluid scaling behavior over a broad intermediate temperature range, as shown in Fig. 3(d). The similar two-fluid behavior clearly indicates that the intermediate temperature physics above the charge- $2e$ metal is controlled by the NFL M phase with partial Kondo screening rather than the charge- $2e$ metal. This may have important implications for real materials, where the scaling is often interrupted or even suppressed (f -electron relocalization) by magnetic, superconducting, or other long-range orders. A second observation is that $f(0)$ as a function of J_K is nearly identical to the volume of single-occupied region, as shown by the red line in the inset of Figs. 3(b) and 3(d). This confirms the previous speculation of an intimate relation between the two-fluid “order parameter” and the partial Kondo screening at zero temperature²⁰. The quantum state superposition revealed in the exactly solvable model may also be the microscopic origin of the two-fluid phenomenology widely observed in real heavy fermion materials.

D. Luttinger’s theorem

The Luttinger’s theorem provides an important criterion for Landau’s Fermi liquid description of interacting electron systems^{49–51}. It states that the volume enclosed by the Fermi surface should be equal to the number of conduction electrons per unit cell. Mathematically, it is often quoted as^{41,52–54}

$$V_{\text{LC}} \equiv \frac{2}{\mathcal{N}} \sum_{\mathbf{k}} \theta(\text{Re}G_c(\mathbf{k}, 0)) = n_c, \quad (4)$$

where the factor 2 arises from the up and down spins, and $n_c = \frac{1}{\mathcal{N}} \sum_{\mathbf{k}} \langle n_{\mathbf{k}} \rangle$ is the electron density. For a Fermi liquid metal, $\text{Re}G_c(\mathbf{k}, 0)$ changes its sign only at the Fermi surface by passing through infinity, and hence Eq. (4) reduces to the simple Fermi volume statement. It was later suggested that Eq. (4) can also be applied to systems without quasiparticle poles^{52,55}, such as the Mott insulator. In that case, $\text{Re}G_c(\mathbf{k}, 0)$ changes sign by passing through its zeros, which form a Luttinger surface⁵². However, the Luttinger surface of a Mott insulator was found to depend on the arbitrary choice of μ , such that Eq. (4) only holds with the presence of particle-hole symmetry^{53,56}. This suggests a failure of Eq. (4) and possibly nonexistence of the Luttinger-Ward functional in these strongly correlated systems^{53,54,57}.

Here, we demonstrate based on our model that the naive Fermi volume counting is in fact better than the

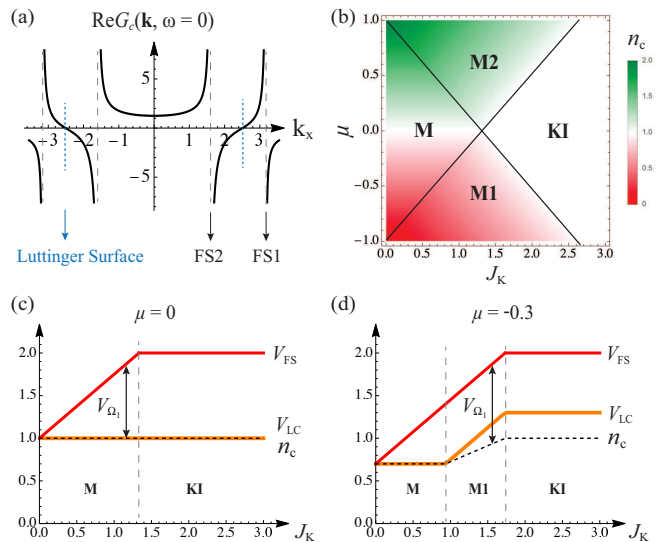


FIG. 4: The Fermi volume evolution and the Luttinger’s theorem. (A) Real part of the Green’s function $G_c(\mathbf{k}, 0)$ at $\mu = 0$, $J_H = 0$, $J_K = 0.8$, showing both the Luttinger surface and the Fermi surfaces (FS1 and FS2). (B) The electron density as a function of μ and J_K at $J_H = 0$. M, M1 and M2 denote different metallic phases, and KI is the Kondo insulator phase. (C)(D) Evolution of V_{FS} , V_{LC} , and n_c with increasing J_K at $\mu = 0$ and -0.3 .

Luttinger count V_{LC} on representing the electron density. As shown in Fig. 4(a), the real part of the Green’s function $\text{Re}G_c(\mathbf{k}, 0)$ at $J_H = 0$ reveals a Luttinger surface inside Ω_1 and two Fermi surfaces at the boundaries of Ω_1 and Ω_2 . Therefore, we can define the Fermi volume as $V_{\text{FS}} \equiv 2(V_{\Omega_1} + V_{\Omega_2})$, and study its relation to the electron density. To do this, we first calculate n_c as a function of J_K and μ at $J_H = 0$. The result is shown in Fig. 4(b). For nonzero μ , there exist another two metallic phases, M1 and M2, where one of the two Fermi surfaces disappears due to the absence of Ω_2 or Ω_0 region. Both M1 and M2 will open a single particle gap by turning on a finite J_H , and become another two charge- $2e$ metals. These phases have qualitatively the same physical properties with their counterparts at $\mu = 0$, and hence will not be discussed in detail.

In Figs. 4(c) and 4(d), we compare V_{LC} and V_{FS} with the electron density n_c as functions of J_K at $\mu = 0$ and $\mu = -0.3$, respectively. At $\mu = 0$, we found $V_{\text{LC}} = n_c = 1$ for both the M and KI phases. On the other hand, V_{FS} evolves continuously from n_c at $J_K = 0$ to $n_c + 1$ in the KI phase. The deviation $V_{\text{FS}} - n_c$ is exactly equal to the volume of Ω_1 . In fact, the identity

$$V_{\text{FS}} \equiv 2(V_{\Omega_1} + V_{\Omega_2}) = n_c + V_{\Omega_1} \quad (5)$$

holds for arbitrary μ and J_K , since the electron density can always be written as $n_c = V_{\Omega_1} + 2V_{\Omega_2}$. Equation (5) correctly accounts for the Fermi surface enlargement due to the Kondo screening effect, an important feature of the Kondo lattice⁵¹. By contrast, the deviation $V_{\text{LC}} - n_c$

depends explicitly on the chemical potential in the M1, M2, and KI phases, as shown in Fig. 4(d) for $\mu = -0.3$. The parabolic free electron dispersion leads to $V_{\text{LC}} = n_c$ in the M phase for all μ , which is generally not true for other forms of $\epsilon_{\mathbf{k}}$. In fact, one can derive analytically (see *Appendix C*)

$$V_{\text{LC}} = n_c + \frac{1}{\mathcal{N}} \sum_{\mathbf{k} \in \Omega_1} \text{sgn}(\epsilon_{\mathbf{k}} - \mu), \quad (6)$$

which points to a general violation of Eq. (4) when Ω_1 is present. However, this equation does not reflect the Fermi surface enlargement due to the Kondo screening effect, and is not as useful as Eq. (5) due to its explicit dependence on $\epsilon_{\mathbf{k}}$ and μ .

It should be noted that Eq. (5) has the same form as the generalized Luttinger sum rule derived in the Schwinger boson formalism of the Kondo lattice, where V_{Ω_1} corresponds to the volume of an emergent holon Fermi surface^{11,12,58}. In both cases, an intermediate phase with $0 < V_{\Omega_1} < 1$ is allowed, featured with partial (nonlocal) Kondo screening of local spins and gapless spinon and holon excitations, which is completely different from the Kondo-destruction scenario where V_{FS} jumps from n_c to $n_c + 1$ through a local QCP. This partial screening in the momentum space should be distinguished from those studied in the coordinate space⁵⁹, which is always accompanied by broken translational symmetry.

III. DISCUSSION

We briefly discuss to what extent our toy model reflects the true physics of correlated f -electron systems. First, the momentum space local spins can be originated from an infinitely large Hatsugai-Kohmoto (HK) interaction between f -electrons, $U \sum_{\mathbf{k}} n_{\mathbf{k}\uparrow}^f n_{\mathbf{k}\downarrow}^f$. Although being a simplification of the Hubbard model, the HK model has recently been shown to capture the essential physics of Mottness and some important high- T_c features upon doping^{41,42}. As suggested in Ref.⁴², this is possibly because the HK interaction is the most relevant part of the Hubbard interaction that drives the system away from the Fermi liquid fixed point to the Mott insulator. In fact, a perfect single-occupancy constraint on every lattice site ($n_i^f = 1$) must also imply the single-occupancy at each momentum point ($n_{\mathbf{k}}^f = 1$). Therefore, we believe our model does capture the essential physics of strongly correlated f -electrons. Second, the Kondo term of our model contains a particular form of nonlocal Kondo interaction proposed in recent Schwinger boson theories of Kondo lattices with strong quantum fluctuation or geometric frustration^{11,12}, $J_K(|\mathbf{r}_i - \mathbf{r}_j|) c_{i\alpha}^\dagger c_{j\beta} f_{j\beta}^\dagger f_{i\alpha}$. It is related to the term $c_{i\alpha}^\dagger \boldsymbol{\sigma}_{\alpha\beta} c_{j\beta} \cdot \mathbf{S}_i \times \mathbf{S}_j$ that emerges naturally upon renormalization group from a Kondo lattice, and may become important in the quantum critical region³⁹.

In summary, we have constructed an exactly solvable Kondo-Heisenberg model in momentum space. This model displays many interesting properties: 1) it realizes a charge- $2e$ metal phase with gapped single particle excitations but gapless Cooper pair excitations; 2) as the Heisenberg interaction vanishes, the charge- $2e$ metal becomes a NFL metal featured with a partially enlarged Fermi volume; 3) both the charge- $2e$ metal and the NFL metal show universal two-fluid behaviors at finite temperatures, reflecting partial Kondo screening of local spins. All these interesting properties arise from the highly non-local Kondo interaction in real space, which might play an important role in heavy fermion systems. Our results may help to understand the experimentally observed NFL quantum critical phase in CePdAl³⁴. For other materials like YbRh₂Si₂, such nonlocal physics might become important in the quantum critical region, causing the smooth evolution of the Fermi surface.

ACKNOWLEDGMENT

This work was supported by the National Natural Science Foundation of China (Grants No. 12174429, No. 11974397), the National Key R&D Program of China (Grant No. 2022YFA1402203), and the Strategic Priority Research Program of the Chinese Academy of Sciences (Grant No. XDB33010100).

Appendix A: Exact diagonalization

The 64-dimensional Hilbert space of $H_{\mathbf{k}}$ can be divided into 9 subspaces according to the electron number $n_{\mathbf{k}}$ and $n_{-\mathbf{k}}$,

$$\begin{aligned} (n_{\mathbf{k}}, n_{-\mathbf{k}}) &= (0, 0), (2, 0), (0, 2), (2, 2) & d = 4 \\ (n_{\mathbf{k}}, n_{-\mathbf{k}}) &= (1, 0), (0, 1), (1, 2), (2, 1) & d = 8 \\ (n_{\mathbf{k}}, n_{-\mathbf{k}}) &= (1, 1) & d = 16 \end{aligned} \quad (\text{A1})$$

where d is the dimension of each subspace. To diagonalize the subspaces, we use the basis $|\phi_{\mathbf{k}} \phi_{-\mathbf{k}} S_{\mathbf{k}}^z S_{-\mathbf{k}}^z\rangle$ to compute the matrix elements, where $\phi_{\mathbf{k}} = 0, \uparrow, \downarrow, 2$ denotes the four electron states and $S_{\mathbf{k}}^z = \uparrow, \downarrow$ denotes the local spin states. The lowest eigenstates within each subspace are listed in Table II. By comparing the lowest eigenenergy $E_{n_{\mathbf{k}}, n_{-\mathbf{k}}}$ of different subspaces, one obtains the ground states of $H_{\mathbf{k}}$ listed in Table I.

Appendix B: Green's function

The retarded single-electron Green's function can be directly calculated from its definition, leading to

$$G_c(\mathbf{k}, \omega) = \sum_n \frac{|\langle n | c_{\mathbf{k}, \alpha}^\dagger | 0 \rangle|^2}{\omega - E_n + E_0} + \sum_n \frac{|\langle n | c_{\mathbf{k}, \alpha} | 0 \rangle|^2}{\omega + E_n - E_0}, \quad (\text{B1})$$

TABLE II: The eigenstates of $H_{\mathbf{k}}$ with the lowest energy $E_{n_{\mathbf{k}}, n_{-\mathbf{k}}}$ in each subspace labelled by $(n_{\mathbf{k}}, n_{-\mathbf{k}})$. For simplicity, the states are not normalized. The eigenstates for the $(2, 0), (0, 1), (2, 1)$ subspaces can be obtained from those of $(0, 2), (1, 0), (1, 2)$ by a symmetry transformation $\mathbf{k} \leftrightarrow -\mathbf{k}$. We have defined $\tilde{J} = \sqrt{J_H^2 - 2J_H J_K + 4J_K^2}$ and $\tilde{J}' = \sqrt{J_H^2 - J_H J_K + J_K^2}$.

$(n_{\mathbf{k}}, n_{-\mathbf{k}})$	$E_{n_{\mathbf{k}}, n_{-\mathbf{k}}}$	Eigenstate
(0,0)	$-\frac{3}{4}J_H$	$ 00 \uparrow\downarrow\rangle - 00 \downarrow\uparrow\rangle$
(0,2)	$2(\epsilon_{\mathbf{k}} - \mu) - \frac{3}{4}J_H$	$ 02 \uparrow\downarrow\rangle - 02 \downarrow\uparrow\rangle$
(2,2)	$4(\epsilon_{\mathbf{k}} - \mu) - \frac{3}{4}J_H$	$ 22 \uparrow\downarrow\rangle - 22 \downarrow\uparrow\rangle$
(1,0)	$\epsilon_{\mathbf{k}} - \mu - \frac{J_H + J_K + 2\tilde{J}'}{4}$	$(J_K + \tilde{J}' - J_H)(\uparrow 0 \downarrow\downarrow\rangle - \downarrow 0 \uparrow\downarrow\rangle) - J_H(\downarrow 0 \uparrow\downarrow\rangle - \downarrow 0 \downarrow\uparrow\rangle)$ $(J_H + \tilde{J}' - J_K)(\uparrow 0 \uparrow\downarrow\rangle - \uparrow 0 \downarrow\uparrow\rangle) - J_K(\uparrow 0 \downarrow\uparrow\rangle - \downarrow 0 \uparrow\uparrow\rangle)$
(1,2)	$3(\epsilon_{\mathbf{k}} - \mu) - \frac{J_H + J_K + 2\tilde{J}'}{4}$	$(J_K + \tilde{J}' - J_H)(\uparrow 2 \downarrow\downarrow\rangle - \downarrow 2 \uparrow\downarrow\rangle) - J_H(\downarrow 2 \uparrow\downarrow\rangle - \downarrow 2 \downarrow\uparrow\rangle)$ $(J_H + \tilde{J}' - J_K)(\uparrow 2 \uparrow\downarrow\rangle - \uparrow 2 \downarrow\uparrow\rangle) - J_K(\uparrow 2 \downarrow\uparrow\rangle - \downarrow 2 \uparrow\uparrow\rangle)$
(1,1)	$2(\epsilon_{\mathbf{k}} - \mu) - \frac{J_K + \tilde{J}}{2} - \frac{J_H}{4}$	$2J_K(\uparrow\downarrow\rangle - \downarrow\uparrow\rangle)_{\mathbf{k}}(\uparrow\downarrow\rangle - \downarrow\uparrow\rangle)_{-\mathbf{k}} + (J_H + \tilde{J} - 2J_K)(\uparrow\downarrow\rangle - \downarrow\uparrow\rangle)(\uparrow\downarrow\rangle - \downarrow\uparrow\rangle)$

where ω represents $\omega + i0^+$, and $|n\rangle$ is the n -th eigenstate of $H_{\mathbf{k}}$ with energy E_n . The explicit analytical results are

$$G_c(\mathbf{k} \in \Omega_0, \omega) = \frac{(2\tilde{J}' + 2J_H - J_K)/4\tilde{J}'}{\omega - \epsilon_{\mathbf{k}} + \mu + \frac{J_K - 2J_H + 2\tilde{J}'}{4}} + \frac{(2\tilde{J}' - 2J_H + J_K)/4\tilde{J}'}{\omega - \epsilon_{\mathbf{k}} + \mu + \frac{J_K - 2J_H - 2\tilde{J}'}{4}}, \quad (\text{B2})$$

$$G_c(\mathbf{k} \in \Omega_2, \omega) = \frac{(2\tilde{J}' + 2J_H - J_K)/4\tilde{J}'}{\omega - \epsilon_{\mathbf{k}} + \mu - \frac{J_K - 2J_H + 2\tilde{J}'}{4}} + \frac{(2\tilde{J}' - 2J_H + J_K)/4\tilde{J}'}{\omega - \epsilon_{\mathbf{k}} + \mu - \frac{J_K - 2J_H - 2\tilde{J}'}{4}}, \quad (\text{B3})$$

$$G_c(\mathbf{k} \in \Omega_1, \omega) = \frac{[(\tilde{J} + \tilde{J}')^2 - J_K^2]/8\tilde{J}\tilde{J}'}{\omega - \epsilon_{\mathbf{k}} + \mu - \frac{J_K + 2\tilde{J} - 2\tilde{J}'}{4}} + \frac{[(\tilde{J} + \tilde{J}')^2 - J_K^2]/8\tilde{J}\tilde{J}'}{\omega - \epsilon_{\mathbf{k}} + \mu + \frac{J_K + 2\tilde{J} - 2\tilde{J}'}{4}} + \frac{[J_K^2 - (\tilde{J} - \tilde{J}')^2]/8\tilde{J}\tilde{J}'}{\omega - \epsilon_{\mathbf{k}} + \mu - \frac{J_K + 2\tilde{J} + 2\tilde{J}'}{4}} + \frac{[J_K^2 - (\tilde{J} - \tilde{J}')^2]/8\tilde{J}\tilde{J}'}{\omega - \epsilon_{\mathbf{k}} + \mu + \frac{J_K + 2\tilde{J} + 2\tilde{J}'}{4}}. \quad (\text{B4})$$

For the two-particle Green's function, we have

$$G_b(\mathbf{k}, \omega) = \sum_n \frac{|\langle n | b_{\mathbf{k}}^\dagger | 0 \rangle|^2}{\omega - E_n + E_0} - \sum_n \frac{|\langle n | b_{\mathbf{k}} | 0 \rangle|^2}{\omega + E_n - E_0}, \quad (\text{B5})$$

where $b_{\mathbf{k}}^\dagger = \frac{1}{\sqrt{2}}(c_{\mathbf{k}\uparrow}^\dagger c_{-\mathbf{k}\downarrow}^\dagger - c_{\mathbf{k}\downarrow}^\dagger c_{-\mathbf{k}\uparrow}^\dagger)$ is the Cooper pair creation operator. The analytical results are

$$G_b(\mathbf{k} \in \Omega_0, \omega) = \frac{(\tilde{J} + J_H - J_K)/2\tilde{J}}{\omega - 2(\epsilon_{\mathbf{k}} - \mu) + \frac{J_K - J_H + \tilde{J}}{2}} + \frac{(\tilde{J} - J_H + J_K)/2\tilde{J}}{\omega - 2(\epsilon_{\mathbf{k}} - \mu) + \frac{J_K - J_H - \tilde{J}}{2}}, \quad (\text{B6})$$

$$G_b(\mathbf{k} \in \Omega_2, \omega) = -\frac{(\tilde{J} + J_H - J_K)/2\tilde{J}}{\omega - 2(\epsilon_{\mathbf{k}} - \mu) - \frac{J_K - J_H + \tilde{J}}{2}} - \frac{(\tilde{J} - J_H + J_K)/2\tilde{J}}{\omega - 2(\epsilon_{\mathbf{k}} - \mu) - \frac{J_K - J_H - \tilde{J}}{2}}, \quad (\text{B7})$$

$$G_b(\mathbf{k} \in \Omega_1, \omega) = \frac{(\tilde{J} + J_H - J_K)/2\tilde{J}}{\omega - 2(\epsilon_{\mathbf{k}} - \mu) - \frac{J_K - J_H + \tilde{J}}{2}} - \frac{(\tilde{J} + J_H - J_K)/2\tilde{J}}{\omega - 2(\epsilon_{\mathbf{k}} - \mu) + \frac{J_K - J_H + \tilde{J}}{2}}. \quad (\text{B8})$$

Appendix C: Luttinger's theorem

In the limit $J_H = 0$, the Green's functions (B2)-(B4) reduce to

$$G_c(\mathbf{k}, \omega)^{-1} = \begin{cases} \omega - \epsilon_{\mathbf{k}} + \mu - \frac{3J_K^2/16}{\omega - (\epsilon_{\mathbf{k}} - \mu - J_K/2)}, & \mathbf{k} \in \Omega_0 \\ \omega - \epsilon_{\mathbf{k}} + \mu - \frac{3J_K^2/16}{\omega - (\epsilon_{\mathbf{k}} - \mu + J_K/2)}, & \mathbf{k} \in \Omega_2 \\ \omega - \epsilon_{\mathbf{k}} + \mu - \frac{9J_K^2/16}{\omega - (\epsilon_{\mathbf{k}} - \mu)}, & \mathbf{k} \in \Omega_1 \end{cases} = \omega - \epsilon_{\mathbf{k}} + \mu - \Sigma_c(\mathbf{k}, \omega). \quad (\text{C1})$$

The electron density is related to the time-ordered Green's function via

$$n_c = \frac{2}{\mathcal{N}} \sum_{\mathbf{k}} \int_{-\infty}^{\infty} \frac{d\omega}{2\pi} G_c(\mathbf{k}, i\omega) e^{i\omega 0^+} \quad (\text{C2})$$

where we have performed a wick rotation $\omega + i0^+ \rightarrow i\omega$ from Eq. (C1) to obtain the time-ordered Green's function. In proving the Luttinger's theorem, one uses the following identity,

$$G_c(\mathbf{k}, i\omega) = \frac{\partial}{\partial i\omega} \ln G_c(\mathbf{k}, i\omega)^{-1} + G_c(\mathbf{k}, i\omega) \frac{\partial}{\partial i\omega} \Sigma_c(\mathbf{k}, i\omega), \quad (\text{C3})$$

which directly follows from the Dyson's equation (C1). Substituting the first term of the right-hand-side of Eq. (C3) into Eq. (C2) gives exactly the Luttinger's theorem Eq. (4). Therefore Eq. (4) is satisfied if and only if the following integral,

$$\begin{aligned} I_2 &\equiv \frac{2}{\mathcal{N}} \sum_{\mathbf{k}} \int_{-\infty}^{\infty} \frac{d\omega}{2\pi} G_c(\mathbf{k}, i\omega) \frac{\partial}{\partial i\omega} \Sigma_c(\mathbf{k}, i\omega) \\ &= n_c - V_{LC}, \end{aligned} \quad (\text{C4})$$

vanishes, which was proved by Luttinger and Ward to be true to all orders of perturbation theory⁴⁹. However, in our case, from Eq. (C1) and the following identity,

$$\int_{-\infty}^{\infty} \frac{d\omega}{2\pi} \frac{1}{i\omega - A} \frac{1}{(i\omega - B)^2} = \frac{\text{sgn}(B) - \text{sgn}(A)}{2(A - B)^2}, \quad (\text{C5})$$

one can derive $I_2 = -\frac{1}{\mathcal{N}} \sum_{\mathbf{k} \in \Omega_1} \text{sgn}(\epsilon_{\mathbf{k}} - \mu)$, which is generally nonzero. This may originate from the nonexistence of the Luttinger-Ward functional for our system, similar to the cases studied in Refs.^{53,54}.

In fact, for any strictly monotonically increasing function $\epsilon_{\mathbf{k}} = \epsilon(k)$ within the range $k \in [0, 2\sqrt{\pi}]$, one has

$$\begin{aligned} I_2 &= \frac{1}{2\pi} \int_{\max[\epsilon(0), \mu - \frac{3J_K}{4}] }^{\mu} \frac{\epsilon^{-1}(x)}{\epsilon'(\epsilon^{-1}(x))} dx \\ &\quad - \frac{1}{2\pi} \int_{\mu}^{\min[\epsilon(2\sqrt{\pi}), \mu + \frac{3J_K}{4}]} \frac{\epsilon^{-1}(x)}{\epsilon'(\epsilon^{-1}(x))} dx, \end{aligned} \quad (\text{C6})$$

where $\epsilon'(x)$ and $\epsilon^{-1}(x)$ are the derivative and inverse of the function $\epsilon(x)$, respectively. For a parabolic dispersion function $\epsilon(x) = ax^2 + b$, one has $\epsilon^{-1}(x) = \sqrt{(x-b)/a}$ and $\epsilon'(x) = 2ax$, so that

$$I_2 = \begin{cases} \frac{1}{2\pi} \left(\int_{\mu - \frac{3J_K}{4}}^{\mu} - \int_{\mu}^{\mu + \frac{3J_K}{4}} \right) \frac{1}{2a} dx = 0, & \text{M} \\ \frac{1}{2\pi} \left(\int_b^{\mu} - \int_{\mu}^{4\pi a + b} \right) \frac{1}{2a} dx = \frac{\mu - b}{2\pi a} - 1, & \text{KI} \end{cases} \quad (\text{C7})$$

consistent with our numerical results for $a = 1/(2\pi)$ and $b = -1$.

-
- * yifeng@iphy.ac.cn
- ¹ O. Stockert, F. Steglich, Unconventional Quantum Criticality in Heavy-Fermion Compounds. *Annu. Rev. Condens. Matter Phys.* **2**, 79-99 (2011).
 - ² C. Pfleiderer, Superconducting phases of f -electron compounds. *Rev. Mod. Phys.* **81**, 1551 (2009).
 - ³ Y.-F. Yang, An emerging global picture of heavy fermion physics. *J. Phys. Condens. Matter* **35**, 103002 (2023).
 - ⁴ Q. Si, S. Rabello, K. Ingersent, J. L. Smith, Locally critical quantum phase transitions in strongly correlated metals. *Nature* **413**, 804 (2001).
 - ⁵ P. Coleman, C. Pépin, Q. Si, R. Ramazashvili, How do Fermi liquids get heavy and die?. *J. Phys. Condens. Matter* **13**, R723-R738 (2001).
 - ⁶ T. Senthil, M. Vojta, S. Sachdev, Weak magnetism and non-Fermi liquids near heavy-fermion critical points. *Phys. Rev. B* **69**, 035111 (2004).
 - ⁷ C. Pépin, Fractionalization and Fermi-Surface Volume in Heavy-Fermion Compounds: The Case of YbRh₂Si₂. *Phys. Rev. Lett.* **94**, 066402 (2005).
 - ⁸ I. Paul, C. Pépin, M. R. Norman, Kondo Breakdown and Hybridization Fluctuations in the Kondo-Heisenberg Lattice. *Phys. Rev. Lett.* **98**, 026402 (2007).
 - ⁹ Y. Komijani, P. Coleman, Emergent critical charge fluctuations at the Kondo breakdown of heavy fermions. *Phys. Rev. Lett.* **122**, 217001 (2019).
 - ¹⁰ J. Wang *et al.*, Quantum phase transition in a two-dimensional Kondo-Heisenberg model: A dynamical Schwinger-boson large- N approach. *Phys. Rev. B* **102**, 115133 (2020).
 - ¹¹ J. Wang, Y.-F. Yang, Nonlocal Kondo effect and quantum critical phase in heavy-fermion metals. *Phys. Rev. B* **104**, 165120 (2021).
 - ¹² J. Wang, Y.-F. Yang, Z₂ metallic spin liquid on a frustrated Kondo lattice. *Phys. Rev. B* **106**, 115135 (2022).
 - ¹³ J. Wang, Y.-F. Yang, A unified theory of ferromagnetic quantum phase transitions in heavy fermion metals. *Sci. China-Phys. Mech. Astron.* **65**, 257211 (2022).
 - ¹⁴ J. Wang, Y.-Y. Chang, C.-H. Chung, A mechanism for the strange metal phase in rare-earth intermetallic compounds. *Proc. Natl. Acad. Sci. USA* **119**, e2116980119 (2022).
 - ¹⁵ J.-J. Dong, Y.-F. Yang, Development of long-range phase coherence on the Kondo lattice. *Phys. Rev. B* **106**, L161114 (2022).
 - ¹⁶ S. Nakatsuji, D. Pines, Z. Fisk, Two Fluid Description of the Kondo lattice, *Phys. Rev. Lett.* **92**, 016401 (2004).
 - ¹⁷ N. J. Curro, B.-L. Young, J. Schmalian, D. Pines, Scaling in the emergent behavior of heavy-electron materials, *Phys. Rev. B* **70**, 235117 (2004).
 - ¹⁸ Y.-F. Yang, D. Pines, Universal Behavior in Heavy-Electron Materials, *Phys. Rev. Lett.* **100**, 096404 (2008).
 - ¹⁹ Y.-F. Yang *et al.*, Scaling the Kondo lattice, *Nature* **454**, 611 (2008).
 - ²⁰ Y.-F. Yang, D. Pines, Emergent states in heavy-electron materials, *Proc. Natl. Acad. Sci. USA* **109**, E3060-E3066 (2012).
 - ²¹ K. R. Shirer *et al.*, Long range order and two-fluid behavior in heavy electron materials, *Proc. Natl. Acad. Sci. USA* **109**, E3067-E3073 (2012).
 - ²² Y.-F. Yang, Two-fluid model for heavy electron physics, *Rep. Prog. Phys.* **79**, 074501 (2016).
 - ²³ Y.-F. Yang *et al.*, Magnetic Excitations in the Kondo Liquid: Superconductivity and Hidden Magnetic Quantum Critical Fluctuations, *Phys. Rev. Lett.* **103**, 197004 (2009).
 - ²⁴ Y.-F. Yang, D. Pines, Quantum critical behavior in heavy electron materials, *Proc. Natl. Acad. Sci. USA* **111**, 8398-8403 (2014).
 - ²⁵ Y.-F. Yang, D. Pines, Emergence of superconductivity in heavy electron materials, *Proc. Natl. Acad. Sci. USA* **111**, 18178-18182 (2014).
 - ²⁶ G. Lonzarich, D. Pines, Y.-F. Yang, Toward a new micro-

- scopic framework for Kondo lattice materials, *Rep. Prog. Phys.* **80**, 024501 (2017).
- ²⁷ S. Paschen *et al.*, Hall-effect evolution across a heavy-fermion quantum critical point. *Nature* **432**, 881 (2004).
- ²⁸ H. Shishido, R. Settai, H. Harima, Y. Ōnuki, A Drastic Change of the Fermi Surface at a Critical Pressure in CeRhIn₅: dHvA Study under Pressure. *J. Phys. Soc. Jpn.* **74**, 1103 (2005).
- ²⁹ K. Kummer *et al.*, Temperature-Independent Fermi Surface in the Kondo Lattice YbRh₂Si₂. *Phys. Rev. X* **5**, 011028 (2015).
- ³⁰ Q. Y. Chen *et al.*, Band Dependent Interlayer f-Electron Hybridization in CeRhIn₅. *Phys. Rev. Lett.* **120**, 066403 (2018).
- ³¹ A. M. Sengupta, Spin in a fluctuating field: The Bose (+Fermi) Kondo models. *Phys. Rev. B* **61**, 4041 (2000).
- ³² A. Cai, Q. Si, Bose-Fermi Anderson model with SU(2) symmetry: Continuous-time quantum Monte Carlo study. *Phys. Rev. B* **100**, 014439 (2019).
- ³³ J. Rech, P. Coleman, G. Zarand, O. Parcollet, Schwinger Boson Approach to the Fully Screened Kondo Model. *Phys. Rev. Lett.* **96**, 016601 (2006).
- ³⁴ H. Zhao *et al.*, Quantum-critical phase from frustrated magnetism in a strongly correlated metal. *Nat. Phys.* **15**, 1261 (2019).
- ³⁵ E. Eidelstein, S. Moukouri, A. Schiller, Quantum phase transitions, frustration, and the Fermi surface in the Kondo lattice model. *Phys. Rev. B* **84**, 014413 (2011).
- ³⁶ B. Danu, Z. Liu, F. F. Assaad, M. Raczkowski, Zooming in on heavy fermions in Kondo lattice models. *Phys. Rev. B* **104**, 155128 (2021).
- ³⁷ H. Watanabe, M. Ogata, Fermi Surface Reconstruction without Breakdown of Kondo Screening at Quantum Critical Point. *Phys. Rev. Lett.* **99**, 136401 (2007).
- ³⁸ L. C. Martin, F. F. Assaad, Evolution of the Fermi Surface across a Magnetic Order-Disorder Transition in the Two-Dimensional Kondo Lattice Model: A Dynamical Cluster Approach. *Phys. Rev. Lett.* **101**, 066404 (2008).
- ³⁹ J. Wang, Y.-F. Yang, Spin current Kondo effect in frustrated Kondo systems. *Sci. China-Phys. Mech. Astron.* **65**, 227212 (2022).
- ⁴⁰ Y. Hatsugai, M. Kohmoto, Exactly Solvable Model of Correlated Lattice Electrons in Any Dimensions. *J. Phys. Soc. Jpn.* **61**, 2056-2069 (1992).
- ⁴¹ P. W. Phillips, L. Yeo, E. W. Huang, Exact theory for superconductivity in a doped Mott insulator. *Nat. Phys.* **16**, 1175-1180 (2020).
- ⁴² E. W. Huang, G. L. Nava, P. W. Phillips, Discrete symmetry breaking defines the Mott quartic fixed point. *Nat. Phys.* **18**, 511-516 (2022).
- ⁴³ Y. Zhong, Solvable periodic Anderson model with infinite-range Hatsugai-Kohmoto interaction: Ground-states and beyond. *Phys. Rev. B* **106**, 155119 (2022).
- ⁴⁴ Y. Li, V. Mishra, Y. Zhou, F.-C. Zhang, Two-stage superconductivity in the Hatsugai-Kohmoto-BCS model. *New J. Phys.* **24**, 103019 (2022).
- ⁴⁵ G. Baskaran, An exactly solvable fermion model: spinons, holons and a non-Fermi liquid phase. *Mod. Phys. Lett. B* **5**, 643-649 (1991).
- ⁴⁶ V. N. Muthukumar, G. Baskaran, A toy model of interlayer pair hopping. *Mod. Phys. Lett. B* **8**, 699-706 (1994).
- ⁴⁷ T.-K. Ng, Beyond Fermi-Liquid Theory: the k-Fermi liquids. arXiv [Preprint] (2020). <https://arxiv.org/abs/1910.06602> (accessed 17 January 2020).
- ⁴⁸ A. Kapitulnik, S. A. Kivelson, B. Spivak, Colloquium: Anomalous metals: Failed superconductors. *Rev. Mod. Phys.* **91**, 011002 (2019).
- ⁴⁹ J. M. Luttinger, J. C. Ward, Ground-States Energy of a Many-Fermion System. II. *Phys. Rev.* **118**, 1417 (1960).
- ⁵⁰ J. M. Luttinger, Fermi Surface and Some Simple Equilibrium Properties of a System of Interacting Fermions. *Phys. Rev.* **119**, 1153 (1960).
- ⁵¹ M. Oshikawa, Topological Approach to Luttinger's Theorem and the Fermi Surface of a Kondo Lattice. *Phys. Rev. Lett.* **84**, 3370 (2000).
- ⁵² I. Dzyaloshinskii, Some consequences of the Luttinger theorem: The Luttinger surfaces in non-Fermi liquids and Mott insulators. *Phys. Rev. B* **68**, 085113 (2003).
- ⁵³ T. D. Stanescu, P. Phillips, T.-P. Choy, Theory of the Luttinger surface in doped Mott insulators. *Phys. Rev. B* **75**, 104503 (2007).
- ⁵⁴ K. B. Dave, P. W. Phillips, C. L. Kane, Absence of Luttinger's Theorem due to Zeros in the Single-Particle Green Function. *Phys. Rev. Lett.* **110**, 090403 (2013).
- ⁵⁵ R. M. Konik, T. M. Rice, A. M. Tsvelik, Doped Spin Liquid: Luttinger Sum Rule and Low Temperature Order. *Phys. Rev. Lett.* **96**, 086407 (2006).
- ⁵⁶ A. Rosch, Breakdown of Luttinger's theorem in two-orbital Mott insulators. *Eur. Phys. J. B* **59**, 495-502 (2007).
- ⁵⁷ E. Kozik, M. Ferrero, A. Georges, Nonexistence of the Luttinger-Ward Functional and Misleading Convergence of Skeleton Diagrammatic Series for Hubbard-Like Models. *Phys. Rev. Lett.* **114**, 156402 (2015).
- ⁵⁸ P. Coleman, I. Paul, J. Rech, Sum rules and Ward identities in the Kondo lattice. *Phys. Rev. B* **72**, 094430 (2005).
- ⁵⁹ Y. Motome, K. Nakamikawa, Y. Yamaji, M. Udagawa, Partial Kondo screening in frustrated Kondo lattice systems. *Phys. Rev. Lett.* **105**, 036403 (2010).